# Chain Dynamics and Glass Transition of Dry Native Cellulose Solutions in Ionic Liquids

SCHOLARONE™
Manuscripts

# Chain Dynamics and Glass Transition of Dry Native Cellulose Solutions in Ionic Liquids

Nyalaliska W. Utomo[1], Indira Saifuddin[2], Behzad Nazari[1], Preet Jain[2], and Ralph H. Colby[1]

[1]Department of Materials Science and Engineering

[2]Department of Chemical Engineering,

The Pennsylvania State University, University Park, PA 16802

## Abstract

Dry native cellulose solutions in 1-butyl-3-methylimidazolium methylphosphonate (EMImMPO$_3$H), 1-butyl-3-methylimidazolium acetate (EMImAc), and 1-butyl-3-methylimidazolium chloride (BMImCl) ionic liquids (IL) were investigated using subambient linear viscoelastic oscillatory shear. Glass transition temperatures ($T_g$) of solutions with various cellulose concentrations up to 8.0 wt.% were observed as the peaks of loss tangent tan ($\delta$) and loss modulus $G''$ in descending temperature sweeps at 1 rad/s. Cellulose/IL solutions showed a minimum in $T_g$ at ~2.0 wt.% cellulose content before increasing with cellulose concentration, suggesting a perturbation of the strongly structured IL solvents by the cellulose chains. Isothermal frequency sweeps in the vicinity of $T_g$ were used to construct time-temperature-superposition master curves. The angular frequency shift factor $a_T$ as a function of temperature indicates Arrhenius behavior within a 9 K range near $T_g$, allowing calculation of fragility, which was found to be constant up to 8.0 wt.% cellulose concentration. This result implied that increasing cellulose concentration initially decreases $T_g$ due to disrupted ionic regularity of ILs, but does not seem to change their fragility.

1

**Introduction**

Biopolymers including cellulose are potential future replacements of petroleum-based polymers. As the most abundant biopolymer on Earth, cellulose is produced in hundreds of billions of tons annually, sourced mostly from green plants. The anhydroglucose rings connected by β(1-4) glucosidic linkages in cellulose serve as the structural support in plants[1-4]. Cellulose versatility includes its ability to be shaped into different structures such as fibers, films, and aerogels from solution processing.

However, strong multiple hydrogen bonds between the cellulose chains in the crystal prevent its dissolution in most organic solvents. Derivatization of cellulose is a common method to be able to dissolve it in different solvents, despite the inefficiency and toxicity. Derivatized cellulose usually loses many of its hydrogen bonding -OH groups, causing fibers spun from derivatized cellulose to have approximately half of the modulus of those spun from native cellulose in ionic liquids. The Viscose process is by far the most popular method to manufacture cellulose[5]. However, chemical modification of the cellulose chains is still required and there are many environmental problems posed by the carbon disulfide ($CS_2$) solvent and the by-products of this process[6].

As cellulose is utilized in many different products such as textiles, biomedicine and food, finding a solvent that does not derivatize cellulose is important[3,7]. Ionic liquids (ILs) are promising solvents that can dissolve cellulose without derivatizing it. Several ionic liquids containing ammonium, pyridinium, or imidazolium cations are reportedly able to dissolve cellulose as long as the anions have sufficiently strong hydrogen bond acceptors[8-11]. Cellulose can easily be regenerated with non-solvents such as water, alcohols, and acetone[8-11]. ILs dissolve cellulose by competing for hydrogen bonds that exist between the cellulose chains[12]. ILs also have a vanishingly low vapor pressure, low flammability, and high thermal, chemical, and oxidative

2

stability[13]. ILs can be regenerated for many process cycles, making them "green" solvents and possible excellent replacements for traditional cellulose solvents[9,13].

In order to utilize ionic liquids in more cellulose manufacturing processes, it is important to understand the chain dynamics of cellulose in these solvents. In studying the solutions of cellulose in ILs, many researchers focus on 1-butyl-3-methylimidazolium chloride (BMImCl) and 1-ethyl-3-methylimidazolium acetate (EMImAc) that are reportedly θ-solvents for native cellulose with overlap concentration c* roughly 0.5 wt.% and entanglement concentration $c_e$ about 2.0 wt.% cellulose (for typical $M_w$ = 120 − 140 kg/mol)[8,14,15]. Despite many researchers focusing on the rheology of these solutions, not much detail has been mentioned about chain segmental dynamics and structural aspects of native cellulose in IL solutions.

One of the important aspects that explain chain dynamics is the solution's glass transition temperature $T_g$. The glass transition temperature of cellulose solutions has proven difficult to determine. Many reported the inability to detect $T_g$ of cellulose solutions through Differential Scanning Calorimetry (DSC) due to the instrument's insensitivity to small changes in heat capacity[16-18]. Herein we show that is likely caused by the unusually broad glass transition, spanning 20 K. This broad glass transition seems to be common for cellulose solutions as it was also observed in temperature sweep measurement of a 15 wt.% cellulose/N-Methylmorpholine N-oxide (NMMO) solution[19]. Compared to thermodynamic testing like DSC, peaks of loss tangent tan ($\delta$) and loss modulus $G''$ obtained from oscillatory shear temperature sweeps often reveal crucial information because these peaks are very sensitive to the state of the solution as well as their composition[20].

Previous works on the rheology of cellulose/IL solutions[21-25] have constructed various time-temperature superposition (tTs) master curves in order to explain entanglements between the

cellulose chains and the viscoelastic behavior of the biopolymer in various ILs. So far, none evaluate tTs master curves near the glass transition and evaluate the fragility of these solutions. Angell[27-30] classified glass formers based on their fragility, with the notion that strong liquids, as opposed to fragile ones including most polymers, have stable structures with properties that do not face any significant changes with the liquid-solid phase change that is the glass transition. The dynamic fragility, as explained by Huang and McKenna[27], can be important as it is commonly correlated with structural relaxation[31,32], chemical structure[33-35], vibrational motions[36], and glassy structural recovery[37-39]. Various methods to obtain fragility have been employed before, and either viscoelastic or dielectric master curves constructed near glass transitions can obtain a shift factor as a function of temperature that can quantify how much structural change is seen with changing temperature.

In this work, we improve understanding of the physical state of cellulose in EMImAc and BMImCl by evaluating the solutions' glass transition temperatures and their viscoelastic response near their glass transition. Time-temperature superposition (tTs) master curves and glass transition temperatures at various cellulose concentrations from rheology experiments are reported in this paper. We investigated the glass transition temperatures of different cellulose concentrations that were reflected by the peaks of loss tangent $\tan(\delta) = G''/G'$ and loss modulus $G''$. The frequency-scale shift factors $a_T$ of various cellulose concentrations near their glass transition temperatures in the two ILs were used to quantify fragility of these solutions. A third ionic liquid that dissolves cellulose, 1-Ethyl-3-methylimidazolium methylphosphonate (EMImMPO$_3$H), was studied using only the temperature at which loss tangent $\tan(\delta)$ shows a maximum, as those solutions let go of the rheometer plates before the lower temperatures at which loss modulus $G''$ would show a maximum.

4

**Materials and methods**

1-Ethyl-3-methylimidazolium acetate (EMImAc) and 1-butyl-3-methylimidazolium chloride (BMImCl) with <50 ppm water were purchased from IOLITEC (Heilbronn, Germany). 1-Ethyl-3-methylimidazolium methylphosphonate (EMImMPO$_3$H) was purchased from Solvionic (Toulouse, France). The viscosity values of the dry, Newtonian ILs are 9.7 Pa.s, 89 mPa.s, and 72 mPa.s at 303 K for BMImCl, EMImAc, and EMImMPO$_3$H respectively. Three cellulose samples (Cell$_{272}$, Cell$_{519}$, and Cell$_{625}$) were provided by Dow Incorporated (Midland, MI) with weight-average molecular weights of 272, 519, and 625 kg/mol; the determination of $M_w$ for these three samples is discussed elsewhere[40]. Prior to sample preparation, ILs were dried in a vacuum oven at 80°C overnight and cellulose was dried in a vacuum oven at 40°C overnight. Cellulose was dissolved in ILs without stirring by keeping the solutions in a vacuum oven at 80°C for ~72 hours. Annealing at 80°C for 20 minutes was done prior to running any test to ensure no moisture in the solutions[41]. Linear viscoelasticity was studied using an ARES-G2 rheometer from TA Instruments (New Castle, DE) equipped with parallel plate geometries with diameters of 3 mm and 8 mm with geometry gap of ~0.5 mm. 3 mm parallel plates were used for glassy conditions (for temperatures ≤ 253 K for cellulose/BMImCl solutions and ≤ 223 K for cellulose/EMImAc solutions) in tTs master curves near $T_g$ and temperature sweep measurements to find $T_g$ of high cellulose concentration samples (c ≥ 1.0 wt.%). 8 mm parallel plates were used for tTs above $T_g$ (T > 223 K for cellulose/EMImAc solutions and T > 253K for cellulose/BMImCl solutions) and for temperature sweep measurements to find $T_g$ of low cellulose concentration samples (c < 1.0 wt.%). Because of the high torque at lower temperatures where peaks of $G''$ were seen, all reported loss modulus $G''$ values were obtained using 3 mm parallel plate geometry while loss tangent tan ($\delta$) values for low concentration samples were measured using 8 mm parallel plate geometry. The

5

ARES-G2 uses a convection oven with flowing dry nitrogen to control system temperature and protect the sample from moisture. Subambient temperature experiments were controlled by a TA Instruments Air Chiller System and Chiller Panel that operates using dried, filtered air. Glass transition temperatures were measured by running downward temperature sweeps at 1 rad/s angular frequency and 1°C/min ramp rate.

**Results and discussion**

*Glass transition temperature*

Oscillatory shear data to determine the glass transition temperature of pure EMImAc are compared to a solution of EMImAc with 7.0 wt.% of $Cell_{625}$ in Fig. 1. Glass transition temperatures were estimated from subambient temperature sweeps at a frequency of 1 rad/s with two $T_g$ defined as the temperatures where there are peaks of loss tangent $\tan(\delta) = G''/G'$ and loss modulus $G''$. The two $T_g$ values obtained from peaks of $\tan(\delta)$ and $G''$ represent the range of temperatures over which the transition between a liquid and a glass happens. Loss tangent $\tan(\delta)$, as seen in Fig. 1, shows a peak at temperatures ~20 K higher than the peak in $G''$, and the values of the two temperatures can be taken as the $T_g$ range of the samples. A ~20 K difference in $G''$ and $\tan(\delta)$ peaks was also seen by Blachot, et al. in 15 wt.% cellulose/NMMO solution through upward temperature sweep measurement[19].

Glassy modulus $G_g$ of order 1 GPa was seen below the glass transition, which was defined as the plateau of storage modulus[20] $G'$ but with 3 mm diameter plates this value is not trustworthy. It is not only difficult to load the sample into the small 3 mm diameter parallel plates perfectly, but 3 mm diameter geometry also tends to cause larger measurement errors due to its compliance contribution to the instrument compliance, therefore requiring a correction in order to obtain an

accurate $G_g$ value[42-44]. Although the $G_g$ values are not reported due to the aforementioned reasons, the temperatures at which $G''$ and tan ($\delta$) have peaks are robust.

The peak in loss modulus $G''$ can be thought of as the temperature where molecular motions start to 'melt' the glass, whereas the ~20 K higher temperature peak in loss tangent tan ($\delta$) is roughly the midpoint of the change in storage modulus from $G_g$ to $G_e$, the entanglement plateau for entangled solutions[45]. The tan ($\delta$) of 7.0 wt.% cellulose/EMImAc is seen to have a wider peak compared to pure EMImAc (Fig. 1) due to ordinary concentration fluctuations from the presence of cellulose chains.
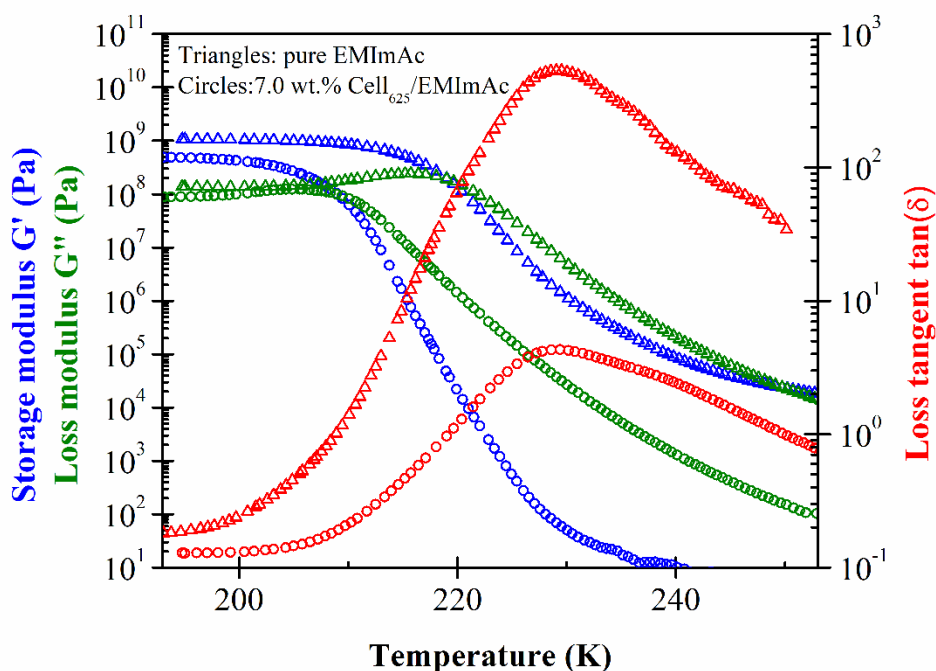


Fig. 1. Downward temperature sweeps at 1 rad/s indicating glass transition temperature ($T_g$) of pure EMImAc (triangles) and 7.0 wt.% Cell$_{625}$/EMImAc solution (circles) with the upper end of $T_g$ defined as the maximum of loss tangent tan ($\delta$) $= G''/G'$ and lower end of $T_g$ defined as the maximum of loss modulus $G''$.

7

From the maxima of $\tan(\delta)$ and $G''$, it can be seen in Fig. 2 that the $T_g$ of 7.0 wt.%

cellulose/BMImCl solutions is considerably higher than cellulose/EMImAc solutions. The

different $T_g$ values between cellulose/BMImCl and EMImAc solutions are caused by the ~33 K

difference in $T_g$ of the two solvents. Yamamuro, et al. reported $T_g$ of BMImCl to be 225 K while

we did not find any reported $T_g$ for EMImAc[46,47]. Our temperature sweep measurements indicate

$T_g$ ranges of pure EMImAc and BMImCl to be 205 K – 229 K and 236 K – 262 K, respectively.

These values are compared to the $T_g$ of 7.0 wt.% cellulose solutions in Table 1. Fox and Flory

reported that for polymers with $M_w < 20$ kg/mol, there is an increase of $T_g$ as molecular weight

increases[48]. Since the $M_w$ of cellulose samples used was well above 20 kg/mol ($272 - 625$ kg/mol),

these solution $T_g$ values are expected to be independent of $M_w$. $Cell_{272}$, $Cell_{519}$, and $Cell_{625}$ have

very similar $T_g$, shown by the overlapping temperature sweep curves in Fig. 2a and b, and
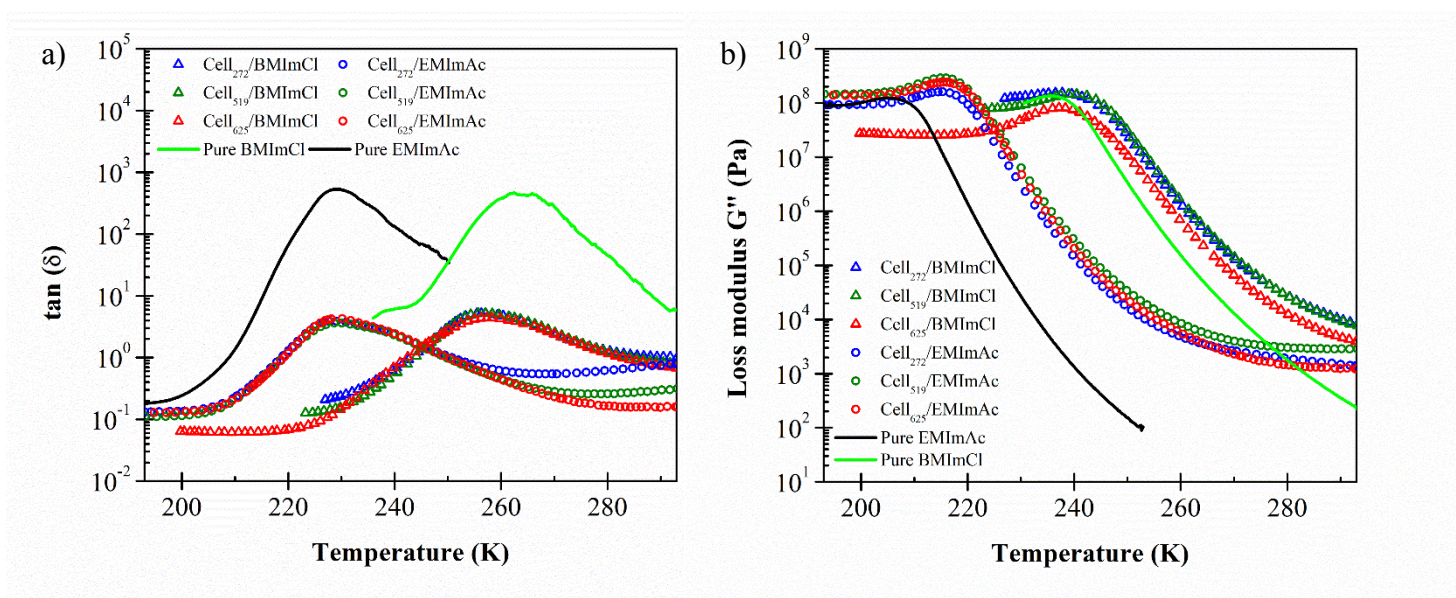
summarized $T_g$ values in Table 1.



Fig. 2. Downward temperature sweeps at 1 rad/s indicating glass transition temperature ($T_g$) of

7.0 wt.% $Cell_{272}$, $Cell_{519}$, and $Cell_{625}$ in BMImCl and EMImAc solutions with $T_g$ as (a) the

maximum of loss tangent $\tan(\delta) = G''/G'$ and (b) as the maximum of loss modulus $G''$. $\tan(\delta)$

and the maximum of loss modulus $G''$ of pure EMImAc and BMImCl are represented by lines.

Table 1. Glass transition temperature ranges of two pure ILs and 7.0 wt.% $Cell_{272}$, $Cell_{519}$, $Cell_{625}$

solutions in the two ILs. $T_g$ were obtained through temperature sweeps and $T_g$ values range from

the maximum of $G''$ (Fig. 2b) to the maximum of $\tan(\delta)$ (Fig. 2a).

| EMImAc | | |
|---|---|---|
| [Cellulose] | $T_g$ (K) from $G''_{max}$ | $T_g$ (K) from $\tan(\delta)_{max}$ |
| 0.0 wt.% | 205 | 229 |
| 7.0 wt.% $Cell_{272}$ | 215 | 229 |
| 7.0 wt.% $Cell_{519}$ | 216 | 230 |
| 7.0 wt.% $Cell_{625}$ | 216 | 229 |
| BMImCl | | |
| [Cellulose] | $T_g$ (K) from $G''_{max}$ | $T_g$ (K) from $\tan(\delta)_{max}$ |
| 0.0 wt.% | 236 | 262 |
| 7.0 wt.% $Cell_{272}$ | 237 | 256 |
| 7.0 wt.% $Cell_{519}$ | 240 | 257 |
| 7.0 wt.% $Cell_{625}$ | 237 | 257 |

The $T_g$ values of 7.0 wt.% cellulose in BMImCl range from 238 K ± 1.5 K from the peak in G" to

258 K ± 2.5 K from the peak in tanδ, while 7.0 wt.% cellulose in EMImAc has $T_g$ varying from

213 K ± 4.6 K from the peak in G" to 229 K ± 0.2 K from the peak in tanδ. Below the lower glass

transition temperature that is from the maximum in loss modulus $G''$, the local conformational

arrangements of cellulose chains do not depend on $M_w$ and temperature because long polymer

chains below $T_g$ are at an iso-free-volume state[20,48,49]. A good measure of the breadth of the glass

transition is the full width at half of the maximum value of $\tan(\delta)$, plotted in Fig. 3. The glass

transition broadens as cellulose is added, also seen in Figs. 1 and 2, consistent with concentration

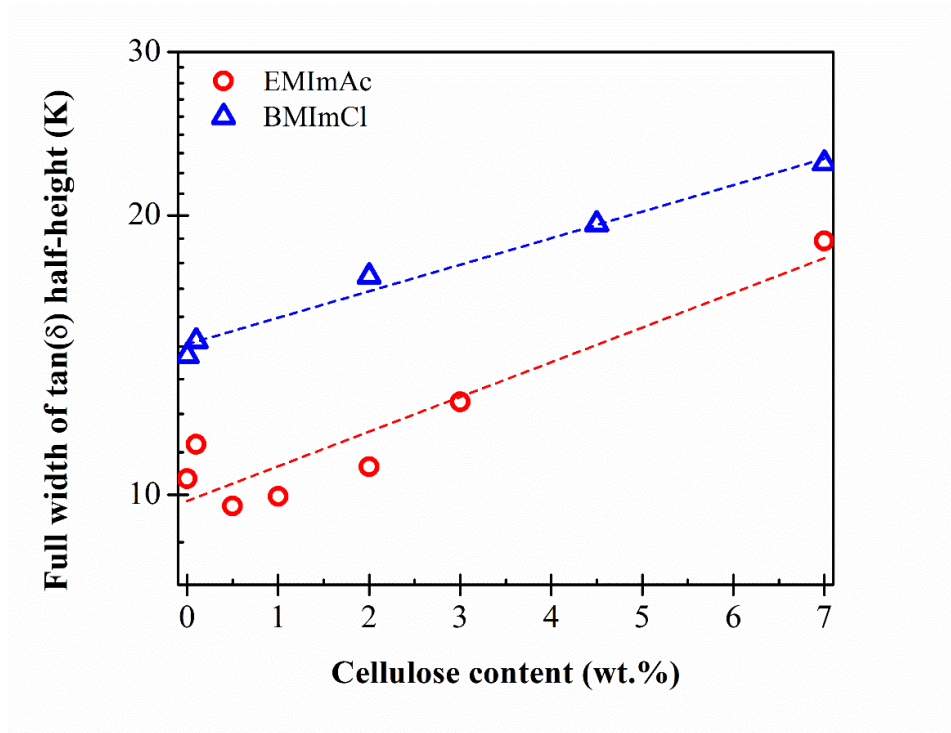fluctuations expected in any polymer solution.

Fig. 3. Cellulose concentration dependence of the breadth of the glass transition, measured as the full-width at half of the maximum of tan ($\delta$) from temperature sweeps like those in Fig. 2a, for solutions of $Cell_{625}$ in BMImCl (blue), EMImAc (red). The glass transition broadens as cellulose is added, as expected from the usual concentration fluctuations.
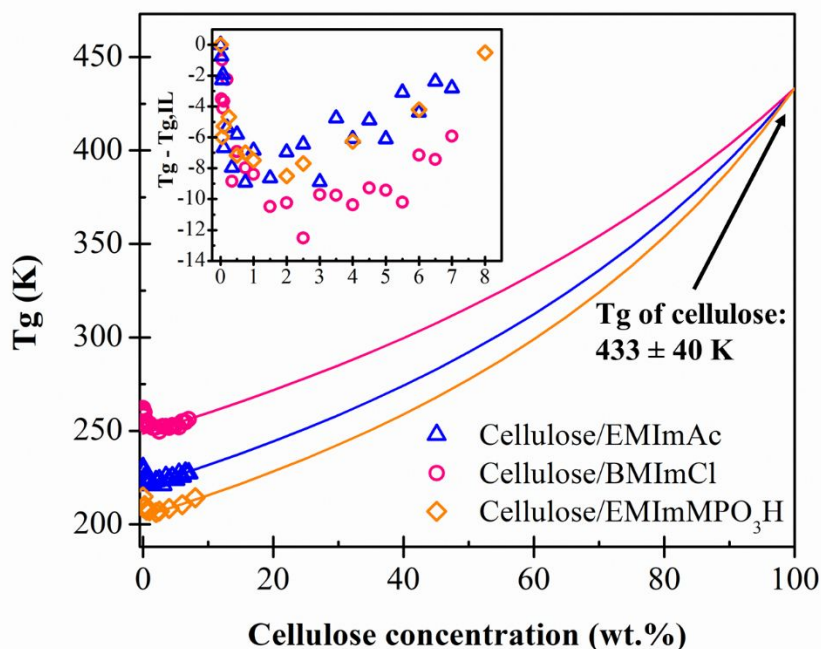
Fig. 4. Glass transition temperature ($T_g$) dependence on $Cell_{625}$ content in BMImCl, EMImAc, and EMImMPO$_3$H solutions. $T_g$ values were obtained from peaks in loss tangent tan ($\delta$) $= G''/G'$ in downward temperature sweeps at 1 rad/s. Fits to Eq. 1 for c > 2.0 wt.% requiring a common $T_g$ = 433 K for pure cellulose are shown as solid curves. The reductions of $T_g$ caused by cellulose addition to the three ionic liquids are compared in the inset.

While the Fox Equation (Eq. 1) suggests that $T_g$ increases with increasing polymer content, Fig. 4 shows that increasing cellulose concentration in all three ionic liquids *decreases* the $T_g$ up to cellulose content of approximately 2.0 wt.%. This nonmonotonic concentration dependence of $T_g$ can clearly be seen from the inset of Fig. 4, where $T_g - T_{g,IL}$ first adopts negative values (the $T_g$ of low concentration solutions have lower than the pure ILs) and reaching a minimum before eventually increasing with addition of cellulose at higher concentrations. We suspect that this is

caused by cellulose disrupting the natural structure of the ILs. Ionic liquids are highly structured

solvents; each cation prefers to be surrounded by anions and vice versa.

The structuring of ionic liquids can be seen from a peak in wide-angle neutron or X-ray

diffraction[50] and also seen in simulations[51-53]. Like many molten salts, ionic liquids are strongly-

coupled ionic systems due to their high ion densities[52,54]. Imidazolium ionic liquids are known to

exhibit three center-of-mass pair distribution function peaks between cation-cation, cation-anion,

and anion-anion[54]. It was reported by Kuang, et al.[54] that the anions and cations of ILs are

connected through strong hydrogen bonding and at the same time, aggregation of alkyl tails on

ILs' cations were observed using dynamic light scattering (DLS) measurements and simulations.

The addition of cellulose disrupts this ionic structure and when this ionic regularity is perturbed,

the broken ionic interactions and added irregularity lowered $T_g$ by $10 - 13$ K in all three ILs.

The addition of solutes with high $T_g$ into a solvent with lower $T_g$ is reflected in an overall increase

in the $T_g$ of solution at higher cellulose concentrations. As the amount of cellulose is increased,

the $T_g$ raises due to the high $T_g$ of cellulose relative to the solvents. The increase in $T_g$ also

indicates the restriction of cellulose chain mobility in solutions due to the limited free volume and

the restrained local relaxation of the ILs. The magnitude of solutions' $T_g$ reflect the value of their

solvent's viscosity; BMImCl has the largest zero-shear viscosity at 303 K and the highest $T_g$,

followed by EMImAc and EMImMPO$_3$H. The Fox Equation (Eq. 1) predicts the solution's $T_g$

using mass fraction $w$ and $T_g$ (in K) of each component, if the $T_g$ of pure cellulose were known.

$$\frac{1}{T_g} = \frac{w_{IL}}{T_{g,IL}} + \frac{w_{cellulose}}{T_{g,cellulose}} \tag{1}$$

Setting the cellulose $T_g = 433$ K allows the solutions in all three ionic liquids with concentration

above 2.0 wt% to fit Eq. 1, yielding the apparent $T_g$'s of pure ILs in Eq. 1 to be determined as

$T_{g,EMImPO_3H} = 204$ K, $T_{g,EMImAc} = 220$ K, and $T_{g,BMImCl} = 248$ K. These apparent $T_g$ values in all

three ILs are within the range of the measured values from Fig. 2a and b (the $T_g$ range for pure

EMImAc is 205 K to 229 K, the $T_g$ range for pure BMImCl is 236 K to 262 K and the $T_g$ range

for pure EMImMPO$_3$H is 201 K to 215 K).  Of course the very long extrapolation done using the

Fox Equation (Eq. 1) with all data above 2.0 wt.%, that suggests a cellulose $T_g$ of 433 K ± 40 K is

not to be trusted since we do not know that the Fox equation is even the right form.  However, the

Fox equation is useful for extrapolating the $T_g$ estimates to higher cellulose concentrations.

Insights toward the physical state through $T_g$ for the normally used $15 - 20$ wt.% cellulose content

in fiber spinning[55-57] could be predicted in these ILs. For fiber spinning solutions with 20 wt.% of

cellulose content, the predicted $T_g$ values according to Fig. 4 are 271 K in BMImCl, 244 K in

EMImAc, and 228 K in EMImMPO$_3$H.

*Time temperature superposition master curves and fragility*

Time-temperature superposition master curves have been constructed for many cellulose/IL

solutions[21-26]. tTs master curves in the literature indicate that cellulose/IL solutions generally

behave like common polymer solutions with a terminal regime and entanglement plateau of $G'$ for

cellulose concentration $c > c_e$ due to chain entanglement[45,58]. At higher concentrations, there are

more cellulose chains present to entangle with one another and the rubbery plateau widens with

increasing cellulose concentration. The results presented so far[21-26], however, did not include any

attempt of measurements in the vicinity of solutions' glass transition temperature. As we intend to

study the fragility of solutions, we extended the tTs master curves to temperatures within the range

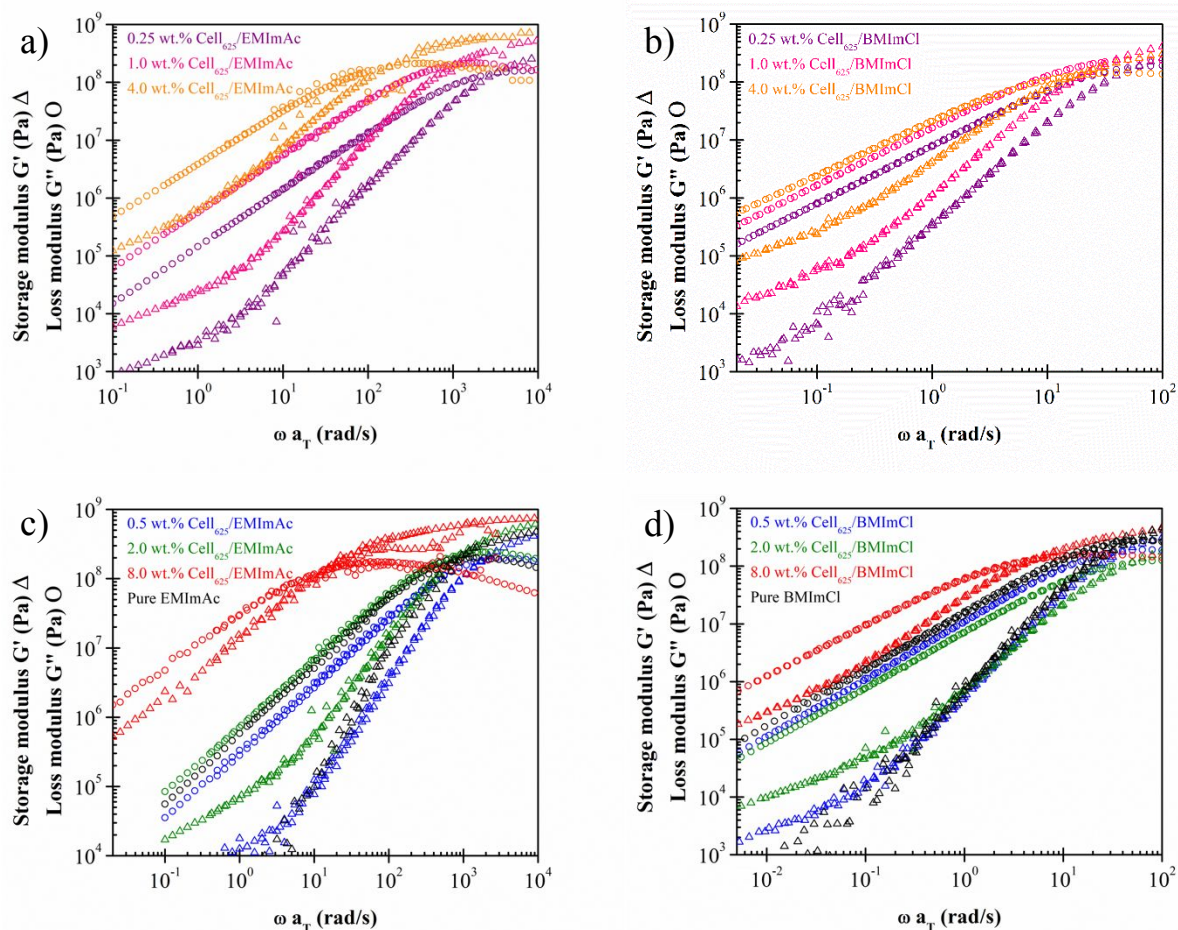of $T_g$ for 0.25, 0.5, 1.0, 2.0, 4.0, and 8.0 wt.% Cell$_{625}$/ILs (Fig. 5).

Fig. 5. Time-temperature superposition (tTs) master curves of 0.25 wt.%, 1.0 wt.%, and 4.0 wt.% Cell$_{625}$ dissolved in (a) EMImAc and (b) BMImCl, and 0.5 wt.%, 2.0 wt.%, and 8.0 wt.% in (c) EMImAc and (d) BMImCl. EMImAc solutions were measured at 214 K to 223 K with reference temperature of 223 K and BMImCl solutions were measured at 244 K to 253 K with reference temperature of 244 K. Pure ILs are indicated by black data points. The lower viscosity (reflected in smaller $G''$ at low frequencies) of the 0.5 wt.% solutions in blue compared with the pure ILs in black is caused by the drop in $T_g$ seen in Fig. 4.

In Fig. 5, the glass transitions of solutions are seen from the maxima of loss modulus $G''$ and the plateauing of storage modulus $G'$ at higher frequencies. At very high frequencies, little to no

14

configurational rearrangements are possible and this develops higher elastic character than its viscous counterpart, often involving stretching and bending of chemical bonds[45]. As previously discussed, polymer chain movements are arrested near the glass transition temperature while at temperatures higher than $T_g$, polymer chains are more mobile. The term also closely related to polymer motion, fragility, is defined by Angell as the change of the base-10 logarithm of solution viscosity with respect to glass transition temperature divided by temperature $(T_g/T)^{28}$. From these definitions, it can be inferred that more fragile solutions will commonly have higher $T_g$[60].
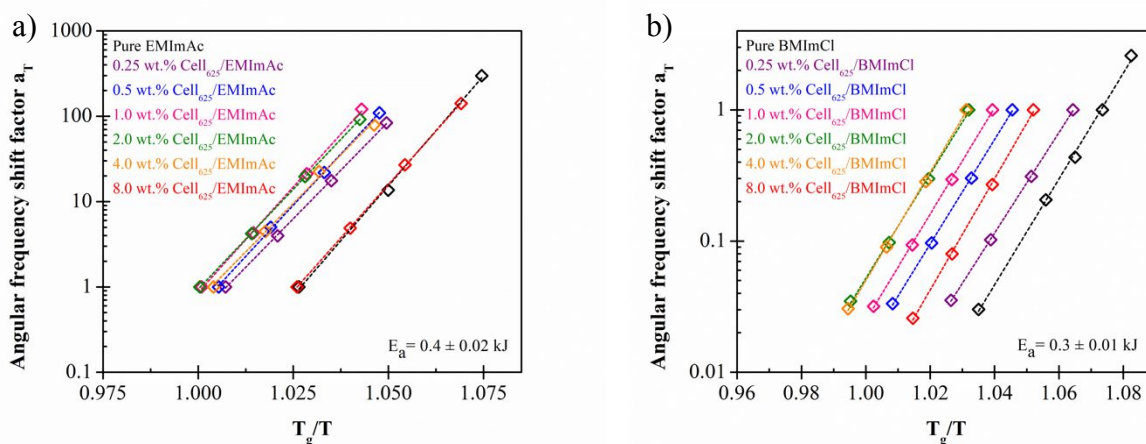


Fig. 6. Shift factor dependence on temperature of 0.0 – 8.0 wt.% cellulose content in (a) EMImAc and (b) BMImCl near $T_g$ shows Arrhenius behavior with similar slope for different concentrations in each solvent. Each shows Arrhenius temperature dependence in the 9 K temperature interval studied, with spacings between the various compositions all about the proximity of the reference temperature to $T_g$.

While constructing the tTs master curves, the angular frequency shift factor $a_T$ was obtained by setting a reference temperature of 223 K for cellulose/EMImAc solutions and 244 K for cellulose/BMImCl solutions. No modulus scale shift factor was utilized $(b_T = 1)$, as $G'$, $G''$ and tan ($\delta$) at the four temperatures superimposed well without having to adjust $b_T$, owing to the 9 K

temperature ranges. By only having angular frequency shift factor $a_T$, the differences between diffusion coefficients in the 9 K temperature range are much more significant than the disparities between the densities at these temperatures[45,60]. The obtained $a_T$ as functions of $T_g/T$ for all solutions in Fig. 6 within the 9 K window are Arrhenius (Eq. 2), where $a_T$ is the angular frequency shift factor, $E_a$ is solution's activation energy, $R$ is the gas constant, $T$ is absolute temperature, and $T_0$ is the chosen reference temperature. Activation energies $E_a$ for Fig. 6 were averaged to $207 \pm 10$ kJ/mol for cellulose/EMImAc solutions and $199 \pm 6$ kJ/mol for cellulose/BMImCl solutions.

$$\log\left(a_T\right) = -\frac{E_a}{2.303R}\left(\frac{1}{T} - \frac{1}{T_0}\right) \tag{2}$$

Over a wider temperature range, the usual non-Arrhenius temperature dependence is observed and within the range of $T_g < T < T_g + 100\ K$, the function can be fit better using the Williams-Landel-Ferry (WLF) equation[55]. A system is said to be more fragile when there is a steeper slope in Fig. 6 at $T_g$. The fragility index $m$ then can be explained as the slope in Fig. 6 at the glass transition temperature ($T_g$), provided by Eq. 3. As seen in Eq. 3, the calculated fragility within the 9 K temperature interval does not depend on the choice of reference temperature $T_0$.

$$m = \left(\frac{\partial \log a_T}{\partial\left(\frac{T_g}{T}\right)}\right)_{T = T_g} \tag{3}$$

Table 2. Glass transition temperature $T_g$ from the peak in tan $(\delta)$, reference temperature $T_0$, and

fragility index $m$ obtained from the temperature dependence of frequency-scale shift factors $a_T$

near $T_g$ (Fig. 6).

| Ionic Liquid | Cellulose content (wt.%) | $T_g$ (K) | $m$ |
|---|---|---|---|
| EMImAc | 0 | 229 | 51.5 |
| | 0.25 | 220 | 45.5 |
| | 0.5 | 221 | 47.9 |
| | 1 | 221 | 49.5 |
| | 2 | 222 | 46.8 |
| | 4 | 224 | 45.4 |
| | 8 | 229 | 50.0 |
| BMImCl | 0 | 262 | 40.4 |
| | 0.25 | 248 | 38.3 |
| | 0.5 | 248 | 39.7 |
| | 1 | 254 | 40.5 |
| | 2 | 250 | 39.7 |
| | 4 | 252 | 41.3 |
| | 8 | 256 | 42.4 |

Solutions of cellulose/EMImAc are more fragile, with an average of $m = 48.1 \pm 2.2$, than

cellulose/BMImCl (Table 2) with an average of $m = 40.3 \pm 1.2$. In good agreement with this result,

fragility for BMImCl with $T_g = 222$ K has been reported by Diogo, et al.[61] through DSC

measurement to be $m = 41$, while from dielectric measurement carried out by Sippel, et al.[62]

BMImCl with $T_g = 228$ K resulted in fragility value of $m = 71$. We found no reported value of

EMImAc fragility, but most imidazolium-based ILs surveyed by Tao, et al.[63] fall into the fragility

range $40 - 80$. Ionic liquids that dissolve cellulose have anions that are good hydrogen bond

acceptors, reflected in Kamlet-Taft $\beta$ parameters larger than $0.85$[10,11,25]. Such strong interactions

perhaps explain why the fragility values reported here are on the low end of the $40 < m < 80$ range

reported for ionic liquids; only the strong ILs can dissolve cellulose.

The different structures of cation and anion in EMImAc and BMImCl obviously cause differences in their fragility indices $m$. Leys, et al.[64] stated that the fragility of ionic liquids depend mostly on the Coulombic forces between the cation and anion. They observed decreasing $m$ with increasing anion size for 1-butyl-3-methylimidazolium ILs, but we see the opposite trend here, with the smaller chloride anion having the smaller fragility.

The large discrepancy between fragility indices of the same glass-forming liquid has commonly been observed by using different methods. Tao, et al.[63] explained that fragility index obtained from DSC usually has a systematic error of $10 - 15\%$ while viscosity measurements are seldom performed close enough to $T_g$ to obtain a reliable fragility index. At the same time, a 5 K change in $T_g$ can easily result in a 20% change in fragility. However, fragilities from DSC and rheology were observed to agree in a narrow temperature range close to $T_g$[63]. Dielectric measurements, on the other hand, include relaxation modes beyond the α-process, and often result in higher fragility values[62]. In our rheology measurements, we extended the temperatures above the solutions' glass transition temperatures with the hope that the fragility indices obtained are more accurate.

Fig. 6 and Table 2 indicate that within the cellulose concentration range up to 8.0 wt.%, there are no significant changes in the values of fragility in each IL. As the fragility stays relatively constant with changing cellulose concentration, it is evident that the trend of glass transition temperature $T_g$ with concentration seen in Fig. 4 is mostly based on the effects that cellulose chains have on ionic regularity in ILs. It is still unclear how solution fragility will change with higher cellulose concentration and whether there will eventually be an increase in fragility with cellulose concentration above 8.0 wt.% cellulose content.

**Conclusions**

Glass transition temperatures of cellulose/EMImAc and cellulose/BMImCl solutions were observed as peaks of loss tangent $\tan(\delta)$ and loss modulus $G''$ in descending temperature sweep measurements. Temperature sweeps of cellulose/ILs solutions over a wide cellulose content revealed that small additions of cellulose initially *decrease* the $T_g$ of solutions as much as ~10 – 13 K up to ~2.0 wt.% cellulose content. This is likely caused by the disruption of ionic regularity of the strongly structured IL solvents by the addition of cellulose chains. At higher concentration, $T_g$ increased towards the $T_g$ of pure cellulose. A very long extrapolation of $T_g$ data for 2.0 wt.% < c < 8.0 wt.% using the Fox equation estimated a value of $T_g = 433$ K $\pm$ 40 K for pure cellulose. Glass transition temperatures of cellulose/IL solutions showed that $T_g$ of cellulose/EMImMPO$_3$H and cellulose/EMImAc solutions are lower than those of cellulose/BMImCl due to the higher $T_g$ of the pure BMImCl solvent.

Fragility indices $m$ of cellulose/IL solutions were calculated from the temperature dependence of angular frequency shift factor $a_T$ within a 9 K temperature range near $T_g$. Arrhenius behavior was observed in $a_T$ and $m$ was larger in value for cellulose/EMImAc ($m = 48.1 \pm 2.2$) compared to cellulose/BMImCl ($m = 40.3 \pm 1.2$). The addition of cellulose in each IL was observed to not change fragility up to 8.0 wt.% cellulose content. Adding cellulose chains into ILs perturbs the ionic regularity of ILs, but does not change ILs' fragility index.

**Conflicts of interest**

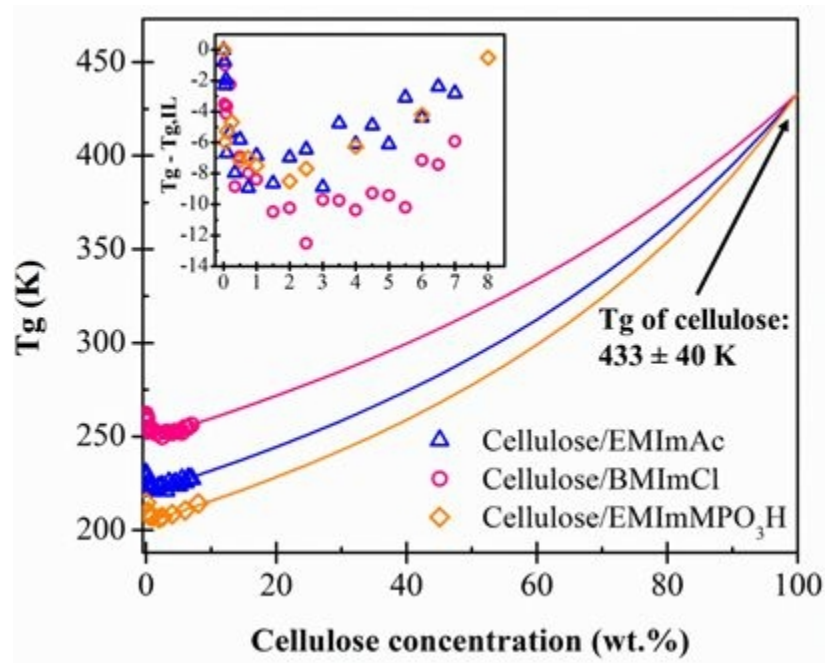There are no conflicts to declare.

**Acknowledgments**

**References**

[1] Sullivan, A. C., *Cellulose*, 1997, **4**(3), 173–207.

[2] Arevalo-Gallegos, A., Ahmad, Z., Asgher, M., Parra-Saldivar, R., Iqbal, H. M., *International Journal of Biological Macromolecules*, 2017, **99**, 308–318.

[3] Umaraw, P., Verma, A. K., *Critical Reviews in Food Science and Nutrition*, 2017, **57**(6), 1270–1279.

[4] Moon, R.J., Martini, A., Nairn, J., Simonsen, J., Youngblood, J., *Chemical Society Reviews*, 2011, **40**, 3941 – 3994.

[5] Polyutov, A. A., Galbraikh, L. S., Byvshev, A. V., Pen, R. Z., Kleiner, Y. Y., Irklei, V. M., *Fibre Chemistry*, 2000, **32**(1), 6–11.

[6] Liebert, T.F., Heinze, T.J., Edgar, K.J., *Cellulose Solvents: For Analysis, Shaping and Chemical Modification*, 2010. Washington, DC: Oxford University Press.

[7] Wang, S., Lu, A., Zhang, L., *Progress in Polymer Science*, 2016, **53**, 169–206.

[8] Swatloski, R. P., Spear, S. K., Holbrey, J. D., Rogers, R. D., *Journal of the American Chemical Society*, 2002, **124**(18), 4974–4975.

[9] Cao, Y., Wu, J., Zhang, J., Li, H., Zhang, Y., He, J., *Chemical Engineering Journal*, 2009, **147**(1), 13–21.

[10] Fukaya, Y., Hayashi, K., Wadab, M., Ohno, H., *Green Chemistry*, 2008, **10**, 44 – 46.

[11] Ohno, H., Fukaya, Y., *Chemistry Letters*, 2009, **38**, 2 – 7.

[12] Pinkert, A., Marsh, K.N., Pang, S., Staiger, M.P., *American Chemical Society*, 2009, **109**, 6712 – 6728.

[13] Zhu, S., Wu, Y., Chen, Q., Yu, Z., Wang, C., Jin, S., Ding, Y., Wu, G., *Green Chemistry*, 2006, **4**, 325 – 327.

[14] Chen, X., Zhang, Y., Wang, H., Wang, S.-W., Liang, S., Colby, R. H., *Journal of Rheology*, 2011, **55**(3), 485–494.

[15] Lu, F., Wang, L., Ji, X., Cheng, B., Song, J., Gou, X., *Carbohydrate Polymers*, 2014, **99**, 132–139.

[16] Szcześniak, L., Rachocki, A., Tritt-Goc, J., *Cellulose*, 2007, **15**(3), 445–451.

[17] Cauley, B. J., Cipriani, C., Ellis, K., Roy, A. K., Jones, A. A., Inglefield, P. T., McKinley, B. J., Kambour, R. P., *Macromolecules*, 1991, **24**(2), 403–409.

[18] Quinn, F. X., Kampff, E., Smyth, G., McBrierty, V. J., *Macromolecules*, 1988, **21**(11), 3191–3198.

[19] Blachot, J.F., Chazeau, L., Cavaille, J.Y., *Polymer*, 2002, **43**, 881–889.

[20] Sperling, L. H., *Introduction to Physical Polymer Science*, 2006, Hoboken: Wiley.

[21] Ahn, Y., Kwak, S., Song, Y., Kim, H., *Physical Chemistry Chemical Physics*, 2016, **18**, 1460-1469.

[22] Lv, Y., Wu, J., Zhang, J., Niu, Y., Liu, C., He, J., Zhang J., *Polymer*, 2012, **53**, 2524-2531.

[23] Haward, S. J., Sharma, V., Butts, C. P., McKinley, G. H., Rahatekar, S. S., *Biomacromolecules*, 2012, **13**, 1688-1699.

[24] Horinaka, J., Yasuda, R., Takigawa, T., *Journal of Polymer Science, Part B: Polymer Physics*, 2011, **49**, 961-965.

[25] Chen, X., Liang, S., Wang, S.-W., Colby, R. H., *Journal of Rheology*, 2018, **62**(1), 81–87.

[26] Choi, U.H., Ye, Y., de la Cruz, D.S., Liu, W., Winey, K.I., Elabd, Y.A., Runt, J., Colby, R.H., *Macromolecules*, 2014, **47**, 777-790.

[27] Huang, D., McKenna, G. B., *The Journal of Chemical Physics*, 2001, **114**(13), 5621–5630.

[28] Angell, C. A., *Journal of Non-Crystalline Solids*, 1985, **73**(1-3), 1–17.

[29] Angell, C. A., *Journal of Non-Crystalline Solids*, 1991, **131-133**, 13–31.

[30] Angell, C. A., *Science*, 1995, **267**(5206), 1924–1935.

[31] Böhmer, R., Ngai, K. L., Angell, C. A., Plazek, D. J., *The Journal of Chemical Physics*, 1993, **99**(5), 4201–4209.

[32] Nemilov, S. V., *Thermodynamic and Kinetic Aspects of the Vitreous State*, 1995. Boca Raton: CRC Press.

[33] Roland, C. M., Ngai, K. L., *Macromolecules*, 1991, **24**(19), 5315–5319.

[34] Ngai, K. L., Roland, C. M., *Macromolecules*, 1993, **26**(25), 6824–6830.

[35] Roland, C. M., *Macromolecules*, 1992, **25**(25), 7031–7036.

[36] Angell, C. A., *Polymer*, 1997, **38**(26), 6261–6266.

[37] Hodge, I. M., *Macromolecules*, 1987, **20**(11), 2897–2908.

[38] Hodge, I. M., *Journal of Non-Crystalline Solids*, 1997, **212**(1), 77–79.

[39] Roland, C. M., Ngai, K. L., *Journal of Non-Crystalline Solids*, 1997, **212**(1), 74-76.

[40] Utomo, N.W., Nazari, B., Colby, R.H., *Cellulose*, "in press".

[41] Nazari, B., Utomo, N. W., Colby, R. H., *Biomacromolecules*, 2017, **18**(9), 2849–2857.

[42] Laukkanen, OV., *Rheologica Acta*, 2017, **56**, 661-671.

[43] Hutcheson, S.A., McKenna, G.B., *Journal of Chemical Physics*, 2008, **129**, 07452.

[44] Schröter, K., Hutcheson, S.A., Shi, X., Mandanici, A., McKenna, G.B., 2006, **125**, 214507.

[45] Ferry, J. D., *Viscoelastic Properties of Polymers*, 1970. New York: Wiley.

[46] Yamamura, O., Minamimoto, Y., Inamura, Y., Hayashi, S., Hamaguchi, H., *Chemical Physics Letters*, 2006, **423**, 371–375.

[47] Sescousse, R., Le, K.A., Ries, M.E., Budtova, T., *The Journal of Physical Chemistry B*, 2010, **114**, 7222–7228.

[48] Fox, T. G., Flory, P. J., *Journal of Applied Physics*, 1950, **21**(6), 581–591.

[49] Strobl, G. R., *The Physics of Polymers*, 1997. Berlin: Springer.

[50] Triolo, A., Mandanici, A., Russina, O., Rodriguez-Mora, V., Cutroni, M., Hardacre, C., Nieuwenhuyzen, M., Bleif, H-J., Keller, L., Ramos, M.A., *Journal of Physical Chemistry B*, 2006, **110**, 21357.

[51] Canongia Lopes, J. N. A., Padua A. A. H., *Journal of Physical Chemistry B*, 2006, **110**, 3330.

[52] Keblinski, P., Eggebrecht, J., Wolf, D., Phillpot, S. R., *The Journal of Chemical Physics*, 2000, **113**(1), 282–291.

[53] Pópolo, M.G.D., Voth, G.A., *Journal of Physical Chemistry*, 2004, **108**, 1744–1752.

[54] Kuang, Q., Zhang, J., Wang, Z. *Journal of Physical Chemistry B*, 2007, **111**, 9858.

[55] Michud, A., Hummel, M., Sixta, H., *Polymer*, 2015, **75**, 1-9.

[56] Bengtsson, J., Jedvert, K., Köhnke, T., Theliander, H., *Journal of Applied Polymer Science*, 2019, **136**(30), 47800.

[57] Zhu, C., Koutsomitopoulou, A.F., Eichhorn, S.J., van Duijneveldt, J.S., Richardson, R.M., Nigmatullin, R., Potter, K.D., *Macromolecular Materials and Engineering*, 2018, **303**(5), 1800029.

[58] Matsumoto, T., Hitomi, C., Onogi, S., *Transactions of the Society of Rheology*, 1975, **19**(4), 541–555.

[59] Qin, Q., McKenna, G.B., *Journal of Non-Crystalline Solids*, 2006, **352**, 2977–2985.

[60] Rubinstein, M., Colby, R. H., *Polymer Physics*, 2003. New York: Oxford University Press Oxford.

[61] Diogo, H.P., Pinto, S.S., Moura Ramos, J.J., *Journal of Molecular Liquids*, 2013, **178**, 142–148.

24

[62] Sippel, P., Lunkenheimer, P., Krohns, S., Thoms, E., Loidl, A., *Scientific Reports*, 2015, **5**, 13922.

[63] Tao, R., Gurung, E., Cetin, M., Mayer, M.F., Quitevis, E.L., Simon, S.L., *Thermochimica Acta*, 2017, **654**, 121–129.

[64] Leys, J., Wubbenhorst, M., Menon, C.P., Rajesh, R., Thoen, J., Glorieux, C., Nockemann, P., Thijs, B., Binnemans, K., Longuemart, S., *Journal of Chemical Physics*, 2008, **128**, 064509.

25

143x116mm (72 x 72 DPI)